J. King Saud Univ., Vol. 19, *Eng. Sci.* (2), pp. 223-237, Riyadh (1427H./2007)

Modeling of Wind Turbine Driving Permanent Magnet Generator with Maximum Power Point Tracking System

Ali M. Eltamaly
Electrical Engineering Department, College of Engineering, King Saud University,
P. O. Box 800, Riyadh 11421, Saudi Arabia
E-mail: eltamaly@ksu.edu.sa

(Received 16 July 2006; accepted for publication 12 December 2006)

Abstract. This paper elaborates on the analysis and simulation of 15 kW Wind Turbine Generator (WTG) driving low speed Permanent Magnet Synchronous Generator (PMSG) using PSIM computer simulation program. The system consists of wind turbine, permanent magnet generator, three-phase diode rectifier, boost converter, and voltage source inverter models. In the WTG model, the best performance coefficient has been determined according to the wind and rotational speed. The low speed PMSG has been used to eliminate gear-box to achieve high efficiency. The ac power output from PMSG is fed to a three-phase diode bridge forward by boost converter to effectively control the dc voltage level. The voltage source PWM inverter is used to interface the system with the electrical utility. The modulation index of the PWM inverter has been controlled to enhance the stability of the dc bus voltage. Simulation results show the superior stable control system and high efficiency.

Keywords: Modeling of wind turbine, Permanent magnet generator, Maximum power point.

List of Symbols

P_m , T_m	: mechanical power and torque production from wind turbine, respectively.
ρ	: air density (kg/m^3).
R	: radius of the swept area by the blades (*m*).
u	: velocity of the wind (*m/sec.*).
C_P , C_T	: power and torque coefficients, respectively.
ω_m	: angular velocity of the shaft (*rad/sec.*).
λ	: tip speed ratio of the WTG.
$V_{d,in}$, $V_{d,out}$	: input and output dc voltage for the boost converter, respectively.
C	: capacitance of the boost capacitor.
V_{LL}	: line to line voltage of PMSG.

D	: duty ratio of boost converter.
t_{on} , t_{off}	: ON and OFF periods of the boost converter, respectively.
$\Delta V_{d,out}$	: peak to peak ripple in the output dc voltage of boost converter.
$I_{d,out}$	: output dc current from boost converter.
f_s , f_{sb}	: switching frequency of the PWM and boost converters, respectively.
T_s	: switch period of the boost converter.
V_{LLC} , V_{LLU}	: line voltages at the leg of PWM inverter and utility grid, respectively.
$\hat{V}_{control}$	: peak amplitude of the control signal.
$\hat{V}_{tri}$	: peak of the triangular signal.
f_1	: fundamental frequency or the frequency of control signal.
h_1 , h_2	: height (m) of measurement and height of the hub of WTG, respectively.
δ	: torque angle at the electric utility side.
X_S	: synchronous reactance of the electric utility.
V_{conv} , V_{ϕ}	: phase voltages at the leg of PWM inverter and utility grid, respectively.

Introduction

As energy demands around the world increase, the need for renewable energy source that will not harm the environment has been also increased. Some projections indicate that the global energy demand will almost triple by 2050. Oil can only supply the world for up to 150 years [1]. Using wind energy is one way to meet the future need. So, it can be said that the wind energy is the fuel of the future. Utilities have the flexibility to accept a contribution of about 20% or more from wind energy systems and more than 50% fuel savings from wind-diesel systems [2]. Hence, it is important to modify the performance of the wind energy systems by modifying the design of mechanical and electrical systems.

This paper plays a significant role in this concept, where the gear-box is replaced by using high efficiency low speed PMSG as shown in Fig. 1. The regular WTG has an induction generator that can rotate at a speed of 1000 to 1700 rpm for normal operation and at reasonable efficiency. This means that a gear-box is needed between the turbine and the induction generator because the regular speed of the WTG before the gear-box is 30-70 rpm. But, in using low-speed PMSG, the rotor rotates at the same speed as the rotor of the turbine. The PMSG can be connected directly to the wind turbine, which results in a simple mechanical system. However, in the tradition system the gear-box adds to the weight, generates noise, demands regular maintenance and increases losses. The maintenance of the gear-box system may be difficult, because the nacelle is located at the top of the tower. Furthermore, there may also be problems with materials, lubrication and bearing seals.

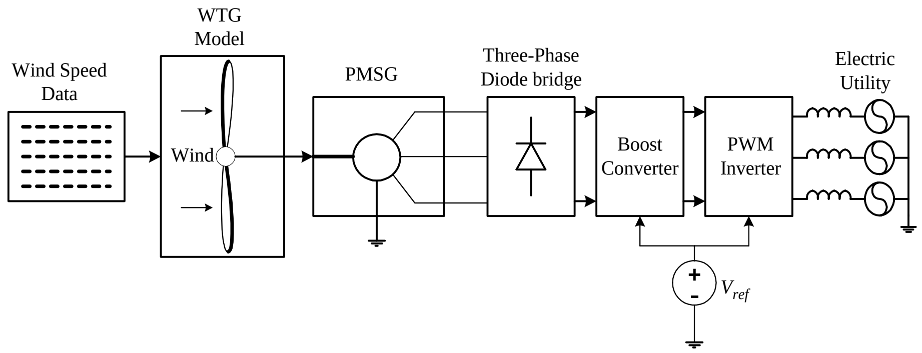

Fig. 1. Modeling of wind turbine driving permanent magnet synchronous generator in PSIM program.

Many disadvantages can also be avoided in gearless WTG. The noise caused mainly by a high rotational speed can be reduced and also high overall efficiency and reliability are achieved in addition to reduced weight and diminished need for maintenance. However, the WTG can extract maximum power at different wind speeds. In the variable speed operation, there is a reduction of the drive train noise, reduction in mechanical stresses, and the increased energy capture.

The mechanical power and torque production from wind turbine is given by [3]:

$$P_m = \frac{1}{2} C_P \rho \pi R^2 u^3 \tag{1}$$

$$T_m = \frac{1}{2} C_T \rho \pi R^3 u^2 \tag{2}$$

where:

P_m , T_m : mechanical power and torque production from wind turbine, respectively.

ρ : air density (kg/m^3).

R : radius of the swept area by the blades (*m*).

u : velocity of the wind (*m/sec*).

C_P , C_T : power and torque coefficients, respectively.

When wind speed changes, the angular velocity of the shaft, ω_m should be adjusted to achieve the best value of C_P . This means that ω_m and the wind speed must somehow be combined into a single variable so that the curve showing the relation between C_P and ω_m can be drawn. Experiments show that this single variable is the ratio of the turbine tip speed $R\omega_m$ to the wind speed *u*. This tip speed ratio, λ is defined as [3]:

$$\lambda = \frac{R\omega_m}{u} \tag{3}$$

where: ω_m is the angular velocity of the shaft (*rad/sec.*).

The relation between C_P, C_T and λ for different kinds of WTG is shown in Fig. 2 [4]. From Eq. (3), it is important to note that the value of power coefficient, C_P and the torque coefficient, C_T are functions of λ, and they are related by $C_T = C_P / \lambda$. From Fig. 2, it is clear that there exists a point where the power coefficient is a maximum. So, in the simulation for different values of wind speed, *u*, the rotational speed, ω_m should be controlled to operate close to $\lambda = 3.8$ (from curve name D in Fig. 2) by controlling active and reactive power delivered to the load. Controlling the duty ratio of the boost converter and the modulation index of the PWM inverter can control active and reactive load power as explained in the design example section.

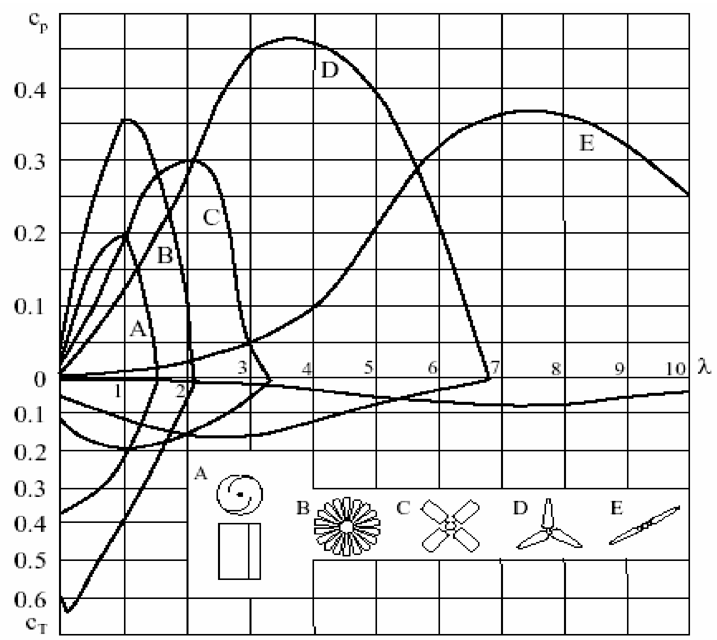

Fig. 2. Power coefficient, C_P and torque coefficient C_T versus λ for different WTG [4].

System Components

The simulation of the system has been carried out by using PSIM computer simulation program [5]. The block diagram of the system is shown in Fig. 1 where the system consists of wind speed data, WTG model (shown in Fig. 3), PMSG, three-phase diode rectifier, boost converter, and three-phase PWM inverter. These components are briefly explained in the following sections.

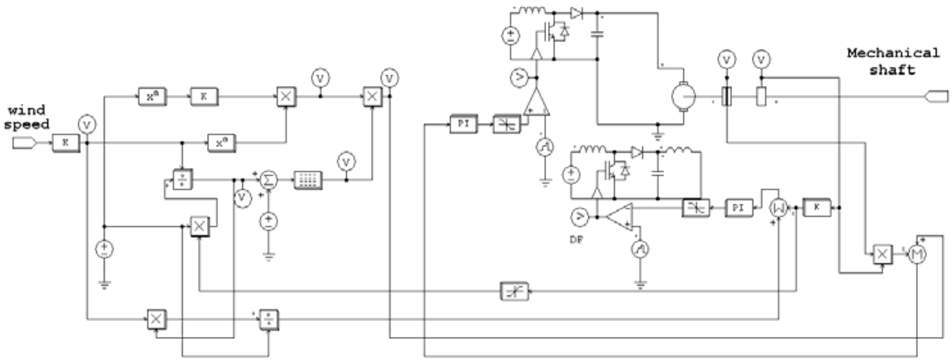

Fig. 3. WTG model by using PSIM computer program.

Three-phase diode bridge rectifier

The diode rectifier is the most simple, cheap, and rugged topology used in power electronic applications. The most disadvantage of this diode rectifier is its disability to work in bi-directional power flow. The output dc voltage from three-phase diode bridge rectifier can be obtained from Eq. (4) where the overlap due to the internal inductance of PMSG is ignored [6].

$$V_{d,in} = \frac{3\sqrt{2}\ V_{LL}}{\pi} \tag{4}$$

where:

$V_{d,in}$: input dc voltage for the boost converter.

V_{LL} : line to line voltage of PMSG.

Step-up (boost) converter

Figure 4 shows a step-up (boost) converter and its control system. As the name implies, the output voltage is always greater than the input voltage. In this model, the boost converter has been controlled to yield constant output dc voltage level, $V_{d,out}$ by varying the duty ratio, D in response to variations in $V_{d,in}$. The relation between the input and output voltage and currents of the boost converter is shown in the following equations [6]:

$$\frac{V_{d,out}}{V_{d,in}} = \frac{1}{(1-D)} \tag{5}$$

$$\frac{I_{d,out}}{I_{d,in}} = (1 - D)$$

where:

$V_{d,out}$: output dc voltage from the boost converter.

D : duty ratio of boost converter.

$I_{d,in}$, $I_{d,out}$: input and output dc current from boost converter, respectively.

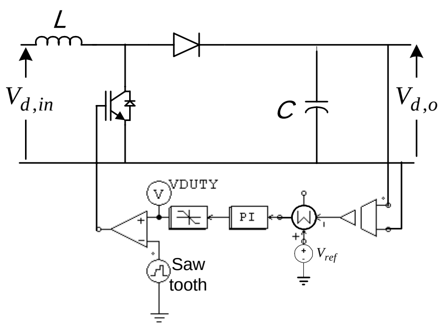

Fig. 4. Step-up dc-dc converter.

The required duty ratio, D as a function of $V_{d,out}/V_{d,in}$ in continuous mode is given by the following equations:

$$D = 1 - \left(\frac{V_{d,in}}{V_{d,out}} \right) \tag{7}$$

The output dc voltage from the boost converter in terms of the input voltage and duty ratio is shown in (8).

$$V_{d,out} = \frac{V_{d,in}}{(1 - D)} \tag{8}$$

Figure 5 shows the steady state waveform of the inductor voltage and current in continuous conduction mode, $[\, i_L(t) > 0 \,]$. The peak to peak ripple of the output dc voltage, $\Delta V_{d,out}$ in continuous conduction mode is given by the following equation [6]:

$$\Delta V_{d,out} = \frac{I_{d,out} D}{C f_{sb}} \tag{9}$$

where;

C : capacitance of the boost capacitor.

f_{sb} : switching frequency of boost converters.

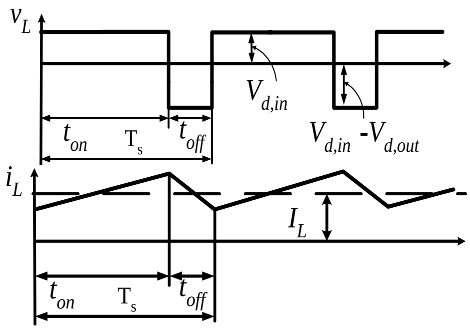

Fig. 5. The waveforms of boost converter.

Pulse width modulation

The first PWM scheme was proposed in 1964 [7]. Since then, there has been intensive research on this topic. All the PWM schemes may be evaluated under a certain switching frequency f_s and the reference signal frequency ratio, and the input to output voltage ratio, which is also named as the modulation index, m_a. The definition of the modulation index, m_a is given by:

$$m_a = \frac{\hat{V}_{control}}{\hat{V}_{tri}} = \frac{\hat{V}_{LLC}}{V_{d,out}} \tag{10}$$

where:

$\hat{V}_{control}$: peak value of the control signal.

$\hat{V}_{tri}$: peak value of the triangular signal.

The frequency modulation ratio m_f is defined as:

$$m_f = \frac{f_s}{f_1} \tag{11}$$

where,

f_s : switching frequency of the PWM inverter.

f_1 : fundamental frequency.

It is always desirable to minimize the distortion of the output voltage and current of the PWM inverter. This distortion increases with increasing the modulation index in the over-modulation region ($m_a > 1$). In the linear region ($m_a \le 1.0$), the fundamental-frequency component in the output voltage varies linearly with the amplitude modulation ratio, m_a as shown in Eq. (10). The line-to-line *rms* voltage at the fundamental frequency at the legs of the PWM inverter, V_{LLC} can be written as [6]:

$$V_{LLC} = \frac{\sqrt{3}}{2\sqrt{2}}\left(m_a V_{d,out}\right) \tag{12}$$

Substituting Eq. (8) into Eq. (12) yields,

$$V_{LLC} = m_a \left[\frac{\sqrt{3} \quad V_{d,in}}{2\sqrt{2}\,(1-D)}\right] \tag{13}$$

In the over-modulation region compared to the linear region ($m_a \le 1.0$), more sideband harmonics appear around the frequencies of harmonics m_f and its multiples. So, careful analysis should ensure that m_a does not exceed one to work in linear region for better control performance and low harmonics in the output voltage and current. Therefore, the power loss in the load due to the harmonic frequencies may not be as high in the over-modulation region as the presence of additional sideband harmonics would suggest.

Design Example

The WTG used in the simulation program has a 4.9-meter radius, 15 kW, 3 blades, 66 rpm rotational speed, 380 V, three-phase PMSG system (see Appendix for details) [8]. Sample of wind speed data of Elzafrana site in Egypt is introduced to the computer program. The wind speed data was measured at about 10 m high. This requires an equation which predicts the wind speed at hub height, $u(h_2)$ in terms of the measured speed at measuring station height, $u(h_1)$. This can be obtained from the following equation [3]:

$$\frac{u(h_2)}{u(h_1)} = \left(\frac{h_2}{h_1}\right)^{1/7} \tag{14}$$

where, h_1, h_2 are heights in meters of measurement and the height of the hub of WTG, respectively.

According to the wind speed and actual rotational speed, the tip speed ratio, λ can be calculated from Eq. (3). From the relation between tip speed ratio, λ and C_P shown in Fig. 2 the value of C_P can be obtained. From the power in the wind and C_P the mechanical power can be calculated from Eq. (1). The mechanical power and the result of multiplying output torque by the ω_m has to be compared. The error signal from this comparison has to be fed to the armature of the dc motor via the boost converter to control the torque. Also, the error signal between the actual rotational speed and the optimum one (at $\lambda = 3.8$) is fed to the field winding of the dc generator via the boost converter to control the shaft speed as shown in Fig. 3.

The mechanical power from the WTG model is fed to the PMSG. The output three-phase voltage of the PMSG is the input for the three-phase diode bridge rectifier. There is no control on the output voltage of the diode bridge rectifier so it can not be connected directly to the PWM because the PWM inverter needs constant dc voltage. So, a controllable dc/dc converter should be used. Depending on the dc output voltage required from the dc/dc converter, boost or buck converter can be used. In this study, the dc output voltage, $V_{d,out}$ is required to be higher than input dc voltage, $V_{d,in}$, so the boost converter is used. By controlling the dc voltage to be constant by controlling the duty cycle of the boost converter and the modulation index of the PWM inverter the maximum available power from the wind can be extracted.

The main drawback of this system is the diode bridge and boost converter are unidirectional power flow devices, so the PMSG has to work only in generator mode which may affect the stability of the system at abnormal conditions. A high capacitance of the dc link capacitor can remedy the effects of this drawback.

The active and reactive powers going to electrical utility are shown in the following equations:

$$P_{out} = 3\left[\frac{V_\phi * V_{conv} * \sin\delta}{X_S}\right] = \left[\frac{V_{LLU} * V_{LLC} * \sin\delta}{X_S}\right] \qquad (15)$$

$$Q_{out} = 3\left[\frac{V_\phi * V_{conv} * \cos\delta - V_{Conv}^2}{X_S}\right] = \left[\frac{V_{LLU} * V_{LLC} * \cos\delta - V_{LLC}^2}{X_S}\right] \qquad (16)$$

By substituting Eq. (13) into Eq. (15) and Eq. (16), the active and reactive power can be obtained in terms of modulation index of PWM inverter and the duty ratio of the boost converter as shown in Eqs. (17) and (18), respectively.

$$P_{out} = \frac{\sqrt{3}\ m_a V_{d,in} V_{LLU} * \sin\delta}{2\sqrt{2}(1-D)X_S} \tag{17}$$

$$Q_{out} = \frac{\sqrt{3}\, m_a\ V_{d,in}}{2\sqrt{2}\,(1-D)\,X_S}\left(V_{LLU} * \cos\delta - \frac{\sqrt{3}\, m_a\ V_{d,in}}{2\sqrt{2}\,(1-D)}\right) \tag{18}$$

where:

δ : torque angle at the electric utility side.

X_S : synchronous reactance of the electric utility.

V_{conv} , V_{ϕ} : phase voltages at the leg of PWM inverter and utility grid, respectively.

It is clear from Eqs. (17) and (18) that the active and reactive power can be controlled by controlling the modulation index, m_a of the PWM inverter and the duty ratio of the boost converter.

Figure 6 shows the time variation of wind speed, u, rotational speed ω_m, output voltage of the diode bridge rectifier $V_{d,in}$, the output voltage of boost converter $V_{d,out}$, the modulation index m_a, the duty ratio D, active output power and P_{out}, reactive output power Q_{out}. Figure 7 shows the diode bridge line current of one phase, the inductor current of boost converter, and the line current going to electric utility. Figure 8 shows the FFT components of diode bridge line current and electrical utility line currents.

It is clear from Fig. 6 and from Eqs. (8) and (12) the proposed system effectively controls the dc link voltage to be around the reference value (730 V). Controlling the dc link voltage to be constant ensures the energy balance between the input and output power.

The proposed system has the following commands:

If $V_{d,out} > 730$ then;	Increase modulation index m_a	Decrease duty ratio D
If $V_{d,out} < 730$ then;	Decrease modulation index m_a	Increase duty ratio D

It is clear from Fig. 8 that the output current from PMSG is highly distorted due to the diode bridge rectifier. This distortion can be easily removed by using third harmonic injection technique [9]. The utility line current has a near sinusoidal shape with very low total harmonic distortion.

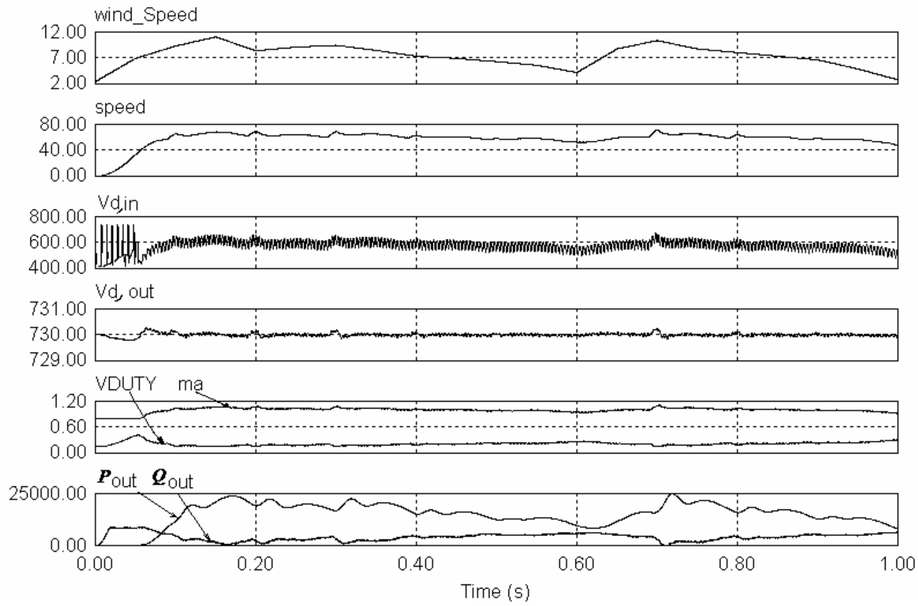

Fig. 6. The time variation of u, N, $V_{d,in}$, $V_{d,out}$, D, m_a, P_{out} and Q_{out}.

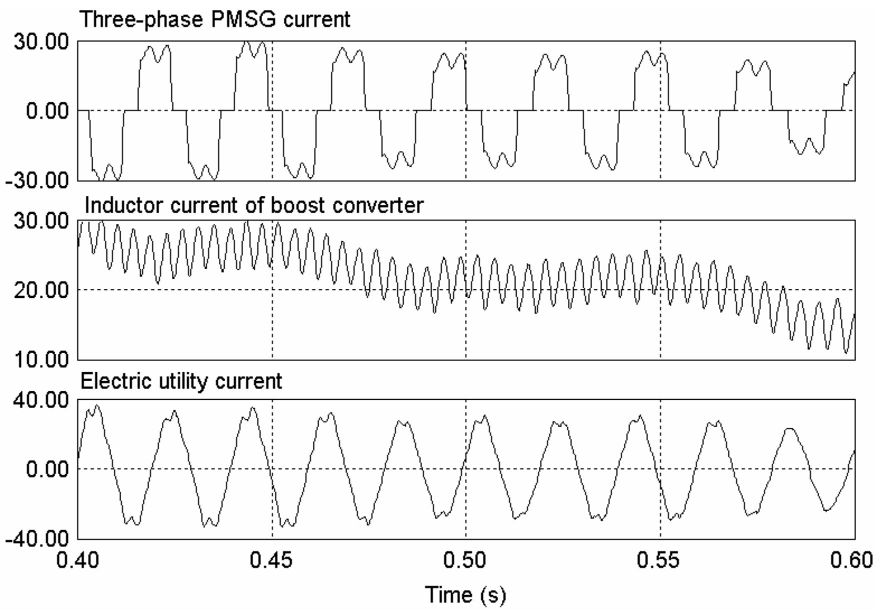

Fig. 7. Diode bridge line current, boost inductor current, and electrical utility line currents.

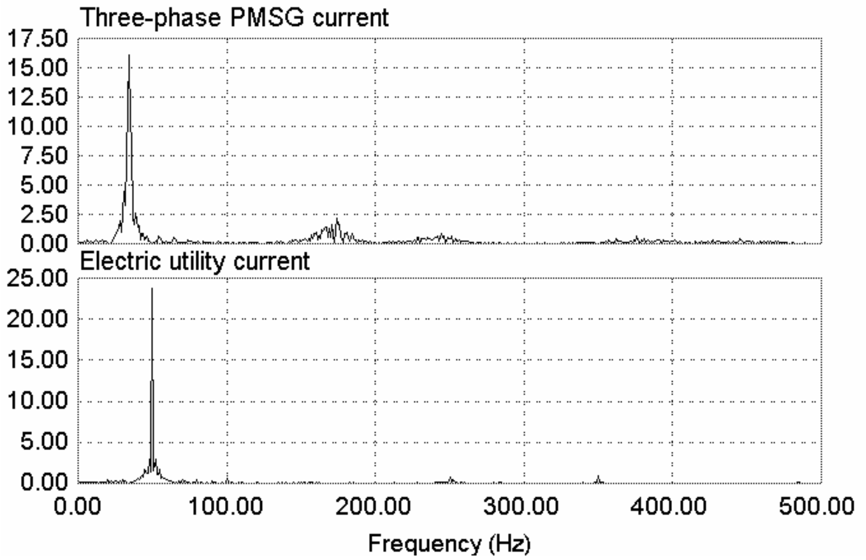

Fig. 8. FFT components of diode bridge line current, and electrical utility line currents.

Conclusion

Modeling and simulation results of a prototype variable speed sensor-less wind energy system is analyzed in this paper. The proposed system does not have self excitation capacitors or gear-box as those used with induction generators. The absence of self excitation capacitors and gear-box translates in reduction in cost, increasing in the efficiency and weight reduction on the nacelle of the WTG. The proposed system utilizes the maximum available power in the wind by forcing the WTG to rotate around the maximum coefficient of performance. The controller is used to achieve the optimal operation at constant dc voltage by controlling the modulation index of PWM inverter and duty ratio of the boost converter to utilize completely the available wind power. The proposed controller has a stable operation for different wind speed. The electrical utility line currents have a very low THD because of the PWM inverter.

References

[1] International Energy Agency Reeport. *Key Issues in Developing Renewable*. 1997.

[2] Battista, H.; Puleston, P. F.; Mantz, R. J. and Christiansen, C. F. "Sliding Mode Control of Wind Energy Systems with DOIG – Power Efficiency and Trosional Dynamics Optimization." *IEEE Trans. on Power System*, 15, No. 2 (May 2000), 728-734.

[3] Johnson, G. L. *Wind Energy Systems*. England Cliffs: Prentic-Hall, 2001.

[4] Fateev, E. M. *Wind Motors and Wind Power Stations*. Moscow, 1948.

[5] PSIM User Manual, refer to this website: www.powerdesign.com.

[6] Mohan, N.; Undeland, T. and Robbins, W. *Power Electronics Converters, Application and Design.* New York: John Wiley & Sons, 2003.

[7] Schonung, A. and Stemmler, H. "Static Frequency Changer with Sub-harmonics Control in Conjunction with Reversible Variable Speed ac Drives." *BBC Review*, Aug./Sep. 1964.

[8] Nacfaire, H. *Grid Connected Wind Turbines*. London and New York: Elsevier Applied Science, 1988.

[9] Eltamaly, Ali M. "A New Relation between Firing Angle of Three-phase SCR Converter and Best Reinjection Current Angle." *The 9th International Middle East Power Systems Conference, MEPCON'2003*, Shebin El-Kom, Egypt, Dec. 2003, 793- 798.

Appendix

The data for dc motor and PMSG generator used in the simulation.

dc motor		**PMSG motor**	
Power	15kW	Power	15 kW
Poles	4	Poles	80
Terminal voltage	200V	Terminal voltage	480V
Rotational speed	75 rpm	Rotational speed	75 rpm
Rated current	50A	Rated current	25A
R_a	0.05 Ω	R_s	2.18 Ω
I_f	4A	L_d	0.0001 H
R_f	75 Ω	L_q	0.0001 H

ذجة توربينة طاقة رياح تدير مولد متزامن دائم ا غنطة مع نظام تتبع للقدرة الأعلى

علي مد التملي

قسم الهندسة الكهربائية، كلية الهندسة، جامعة الملك سعود، ص ب ٨٠٠،
الرياض ١١٤٢١، المملكة العربية السعودية
البريد الإلكتروني: eltamaly@kdu.edu.sa

(قدِّم للنشر في ٢٠٠٥/١٢/٠٣م؛ وقبل للنشر في ٢٠٠٧/٠١/١٣م)

ملخص البحث. يوضح هذا البحث التحليل والمحاكاة لتوربينة طاقة رياح قدرتها ١٥ كيلو واط تدير مولد متزامن دائم المغنطة باستعمال برنامج محاكاة بالحاسوب. تشمل هذه المنظومة توربينة الرياح والمولد المتزامن دائم المغنطة وموحد غير محكوم ثلاثي الطور ومقطع تيار مستمر رافع للجهد وعاكس قدرة للتحويل من التيار الثابت إلى التيار المتردد ثلاثي الطور. تم تتبع أفضل معامل أداء في هذا النموذج بناء على سرعة الرياح وسرعة دوران التوربينة. وتم استعمال المولد المتزامن دائم المغنطة والمنخفض السرعة لإزالة صندوق التروس والحصول على كفاءة عالية. إن القدرة الكهربية المولدة من المولد المتزامن دائم المغنطة تمرر إلى الموحد ثلاثي الطور ثم إلى مقطع التيار المستمر للتحكم في مستوى ثابت للجهد المستمر. تم استخدام عاكس التيار المستمر إلى تيار متردد والذي يعتمد على تعديل عرض الموجة لربط النظام بالشبكة العمومية. تم التحكم بمعامل التعديل للعاكس لكي يحسن استقرار الجهد المستمر، وأظهرت نتائج المحاكاة تفوق وثبات نظام التحكم وكفاءته العالية.